Linking Consistency in Experimental Results to Surface Morphology: A Novel Hypothesis on Laser-Ignited Combustion in Random Particle Packings

Shiquan Lin , Meishuang He , Qijun Liu , Fusheng Liu , Wencan Guo , Hongbo Pei , Xinghan Li *

Posted Date: 9 May 2026

doi: 10.20944/preprints202605.0605.v1

Keywords: laser ignition; random packings; consistency; surface morphology; Discrete Element Model; constrained droplet method

 doi:10.20944/preprints202605.0605.v1

Article

Linking Consistency in Experimental Results to Surface Morphology: A Novel Hypothesis on Laser-Ignited Combustion in Random Particle Packings

Shiquan Lin [1], Meishuang He [1], Qijun Liu [1], Fusheng Liu [1], Wencan Guo [2], Hongbo Pei [2] and Xinghan Li [1,2,*]

[1] School of Physical Science and Technology, Southwest Jiaotong University, Chengdu 610031, China
[2] National Key Laboratory for Shock Wave and Detonation Physics, Mianyang 621900, China
* Correspondence: lixinghan2107@163.com

Abstract

Laser-ignited particle combustion is critical to energy, aerospace, and defense applications, yet understanding its physicochemical mechanisms is hindered by poor reproducibility in combustion data from randomly packed samples. While classical theory attributes data inconsistency to variations in packing density, we propose instead that consistency of the surface layer morphology—given the nanoscale laser penetration depth—is the dominant factor. A two-dimensional Discrete Element Model showed that increasing particle layers markedly reduces surface topography conformity, while gravitational settling maintains packing density near its theoretical maximum. An innovative constrained droplet method was developed for sample preparation, integrating multi-stage sieving, equal-circle packing in a circle theory, alongside droplet deposition to build multilayer samples mirroring computational models. In-situ laser ignition diagnostics revealed that key combustion metrics—spectral profiles, temporal evolution, ignition delay, and combustion duration—exhibit a rapid decline in consistency with increasing layers, closely matching the simulated decay in surface morphology conformity. Contrary to long-held assumptions, this work robustly shows that surface morphology governs laser-ignition experimental reproducibility. This paradigm-shifting finding redefines the controlling mechanism in laser-ignited combustion of random particle packings, thereby provides a method for refining sample preparation and enables the accurate determination of key parameters that remain elusive with conventional approaches.

Keywords: laser ignition; random packings; consistency; surface morphology; Discrete Element Model; constrained droplet method

1. Introduction

Particle combustion is a fundamental phenomenon in natural science and engineering, playing a critical role in energy, chemical industry, aerospace, national defense and other fields [1,2]. Deeper research into its underlying mechanisms is essential for enhancing energy utilization efficiency, optimizing chemical production processes, improving propulsion systems, and advancing the performance of defense-related equipment. As a multidisciplinary problem intersecting chemistry, physics, and materials science, particle combustion is influenced by a range of intrinsic and extrinsic factors. These include particle properties, oxidizer characteristics, atmospheric conditions, physical constraints, and ignition methods [3–5]. Compared with conventional ignition approaches, laser ignition offers distinct advantages such as precise energy delivery, high spatiotemporal resolution, and non-contact operation [6,7]. Furthermore, the ability of lasers to deposit large amounts of energy instantaneously makes them particularly valuable for designing advanced energetic materials [8,9],

 doi:10.20944/preprints202605.0605.v1

where enhanced combustion behavior is of interest. Owing to these capabilities, laser ignition has emerged as a key technique for elucidating the complex physicochemical mechanisms governing particle combustion.

A major challenge in current studies is the poor reproducibility of experimental results obtained from random particle packings. This sample preparation method, which relies on natural gravitational deposition to form multi-layer particle assemblages, typically yields samples with an uncontrolled conical or triangular morphology. Although the use of a metal plate to flatten a sample's top surface is a common preparatory step, the minute scale of the gram-level sample poses a major challenge for quantitatively evaluating its effects. The random packing method has been widely used for its operational simplicity, but it often leads to significant inconsistencies—such as variations in flame spectra and in illumination intensity exceeding 50% between experimental replicates. This high level of deviation fundamentally hinders deeper investigation into the underlying physicochemical mechanisms of the combustion process.

To improve experimental reproducibility, significant research has been devoted to identifying the key factors influencing the consistency of randomly packed samples. A number of studies have attributed the limited reproducibility primarily to the dispersion of packing density. For instance, Beckstead [10], Averardi et al [11], and Nan.y et al [12] linked this inconsistency to inherent variations in packing density within random packings. Bockmon et al [13]. further supported this view by comparing naturally packed samples with pressed ones, noting that the poorer consistency in natural packing arose from its higher packing density dispersion. In particular, Pantoya et al [14] pointed out that packing density lacks controllability, leading to significant inhomogeneity in energy absorption and localized heat conduction pathways. Bharat et al [15] suggested that spatial variation in packing density creates localized hot spots, which lead to amplified statistical scatter in ignition delay and combustion rate. Similarly, Babuk et al [16] argued that loose and irregular packing promotes uneven local combustion and flame propagation, thereby reducing overall combustion consistency. Furthermore, the initial packing density may profoundly influence sintering and agglomeration dynamics. According to Nazarenko et al [17], for nano-aluminum particles, natural packing methods tend to exacerbate random and uneven sintering processes, resulting in unstable combustion wave propagation and poor experimental repeatability. Given these challenges, Kamaraj et al [18] even questioned the scientific reliability of the natural packing method for precise combustion studies.

While the prevailing consensus attributes experimental variability under spatially uniform heating to packing density, the relevance of this factor under laser-ignition conditions—characterized by localized energy concentration and a limited penetration depth—remains an open question. We propose that the similarity of surface layer morphology may play a decisive role in governing experimental reproducibility in laser-induced combustion. Given the nanoscale penetration depth of lasers into opaque particles, the experimental signals predominantly reflect the physicochemical properties of the uppermost layer of the sample at the moment of detection. Among all particle layers, the surface layer exhibits the greatest morphological deviation due to its highest degree of structural freedom. Consequently, deviations in surface morphology can evolve over time during combustion, ultimately leading to significant disparities in observed combustion phenomena. However, classical methodologies often overlook the influence of surface morphology, primarily on the basis that surface particles constitute only a minimal fraction of the entire packed sample.

To uncover the dominant factor controlling experimental reproducibility in laser ignition, we examined the influence mechanisms of both packing density and surface morphology on combustion consistency via a combined methodology of numerical simulation, precision sample fabrication, and experimental validation. This research provides an insightful conclusion that offers a deeper mechanistic understanding of the laser-ignition process.

2. Numerical Calculation

To address the challenge of in-situ morphological characterization for microscale packed samples, we employed a two-dimensional Discrete Element Method (DEM). This approach enables

 doi:10.20944/preprints202605.0605.v1

the simulation of random particle packing, and through repeated sampling and statistical analysis, allows for systematic investigation of how surface morphology and overall packing density evolve as the number of particle layers increases.

The DEM model computed the free fall and subsequent stabilization of numerous two-dimensional spherical particles within a rigid boundary, with initial random placements replicating the randomness inherent in physical sample preparation. The motion of each particle follows Newton's second law :

$$m_i \frac{d\vec{v}_i}{dt} = \sum \vec{F}_i \tag{1}$$

where m_i is the mass of particle i,$\vec{v}_i$ is the velocity vector of particle i. $\sum \vec{F}_i$is the vector sum of all external forces acting on particle i, which is mainly composed of gravity, force between particle i and other particles ($\vec{F}_{ix}$), and force between particle i and rigid boundary ($\vec{F}_{ib}$):

$$\sum \vec{F}_i = m_i \vec{g} + \sum \vec{F}_{ix} + \vec{F}_{ib} \tag{2}$$

where g is the acceleration of gravity. The interactions between particle i and other particles or rigid boundaries were modeled using a classical rigid-body perfect collision model [19] coupled with a damping model. The impulse in the direction of collision (J_i) is given by:

$$J_i = \frac{-(2+e)\vec{v}_i}{\frac{1}{m_i} + \frac{1}{M}} \tag{3}$$

where M represents the mass of the colliding particle or boundary, and e denotes the damping coefficient. This coefficient was incorporated into the force solver to determine the velocity and position of each particle at every time-step. The value of e is inversely related to the damping intensity; a value of e = 0 corresponds to no energy dissipation. Since the primary focus of this study is the final packing characteristics rather than dynamic transients, the damping coefficient was intentionally increased to e= 0.4 to accelerate numerical convergence.

To avoid the formation of poorly controlled and characterized morphologies that result from unrestricted particle accumulation on a flat plate, we conducted two-dimensional numerical simulations of semi-regular multi-layer samples that closely mimic the actual preparation process. Experiments were planned to prepare samples within the inner cavity of a zirconia substrate measuring 2.5 mm in diameter and 2 mm in height. Accordingly, two-dimensional numerical simulations were conducted with a rigid body constraint boundary of 2.5 mm width to investigate the particle arrangement in cross-sections through the cylindrical axis of the sample. Simulations were performed for samples with 1, 2, 3, 4, 5, 10, 20, 30, 40, and 50 packing layers. Given an average particle size of 10 μm, the theoretical number of particles along the sample diameter was calculated to be 250. Consequently, the total number of particles in each simulation was set to 250 multiplied by the number of packing layers. Due to computational constraints when simulating large numbers of layers and particles, only the morphologies for systems with 1 to 4 packing layers were presented in Figure 1, with each configuration repeated five times for statistical reliability.

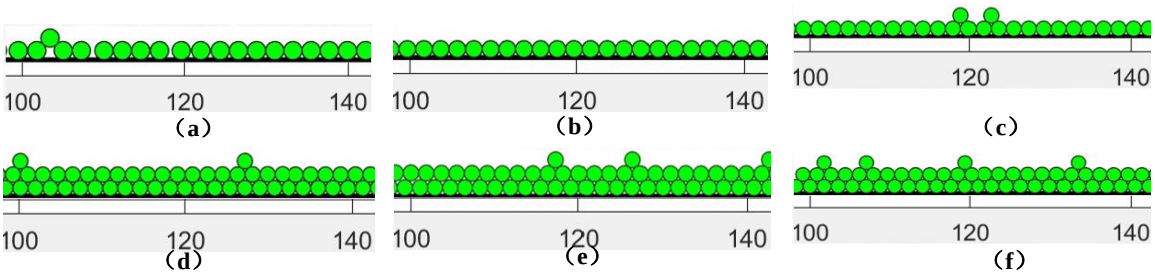

 doi:10.20944/preprints202605.0605.v1

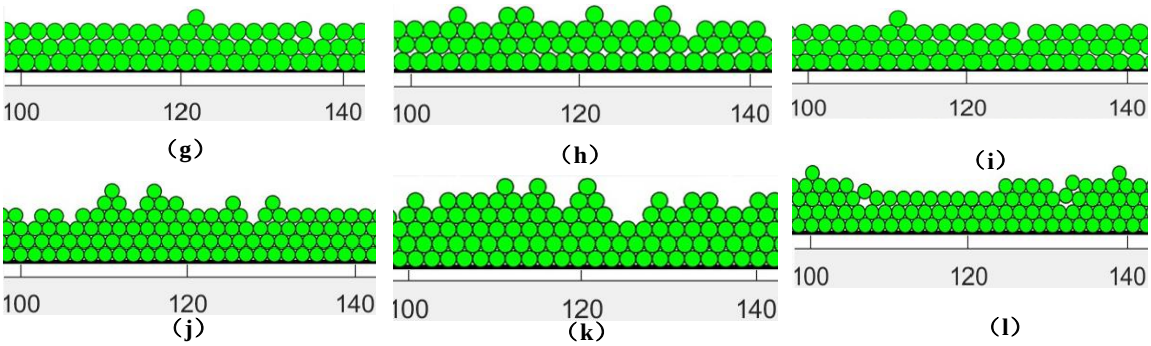

Figure 1. Particle morphology at the midpoint of the packed samples for layer counts of 1 to 4, and the horizontal axis is scaled in units of 10μm. Panels (a) to (c) correspond to results from three independent calculation trials for samples with 1 packing layer. Panels (d) to (f) correspond to results from three independent calculation trials for samples with 2 packing layers. Panels (g) to (i) correspond to results from three independent calculation trials for samples with 3 packing layers. Panels (j) to (l) correspond to results from three independent calculation trials for samples with 4 packing layers.

Figure 1 reveals that under the same number of packing layers, although the simulated packing morphology varies across different calculation runs, key qualitative conclusions can still be drawn. As the number of layers increases, the dispersion of the surface morphology increases significantly, while the variability in the overall packing density remains relatively small. The simulation results indicate that for samples with few layers (≤3 layers), the differences in surface morphology are relatively small, primarily manifesting as isolated particle packing or occasional voids within the first layer, at the scale of single particles. In contrast, for multi-layer packs (≥4 layers), the surface morphology exhibits significantly greater variability, characterized by characteristic random packing features including triangular clusters and elongated particle chains above the first layer, or corresponding voids beneath it, spanning multiple particle diameters. The white inter-particle gaps represent unfilled space, with a higher prevalence of these gaps corresponding to a lower overall packing density. Figure 1 also reveals that the overall packing density does not fluctuate significantly with increasing layer count, as the enhanced gravitational settling effect associated with more layers promotes denser packing.

This study employed a similarity function S to quantitatively characterize surface morphology similarity and the fill factor F to represent overall packing density under identical layer conditions. The S function is a classical method for assessing curve similarity [20], and the conformity of the surface morphology obtained from the i-th trial with the reference morphology was defined as S_i:

$$S_i = e^{-\left|\frac{d^2 f_i(x)}{dx^2} - \frac{d^2 f_0(x)}{dx^2}\right|} \quad (4)$$

where f represents the surface morphology curve, formed by connecting the centers of the first-layer particles in sequence. x is the abscissa, and the subscript 0 designates the reference sample, which is selected from among the multiple calculation runs. S_i equals to 1 corresponding to perfect agreement of the surface morphology in the i-th trial with the reference curve, while a value of 0 signifies that the two are entirely dissimilar.

The filling factor F_i of the i-th trial is defined as:

$$F_i = \frac{N_i \pi R_p^2}{A_i} \quad (5)$$

where N represents the total number of particles, R_P is the particle radius, and A_i is the area of the sample contour. This contour is geometrically defined by the convex hull formed by the centers of the outermost particles along the sample's boundaries. F is the ratio of the total projected area of the particles to A_i. Thus, F is directly proportional to the overall packing density, and F= 1 corresponds to a theoretical condition of perfect, void-free packing. The calculated values of S and F for

 doi:10.20944/preprints202605.0605.v1

different numbers of packing layers of 1、2、3、4、5、10、20、30、40 and 50 are shown in Figure 2.

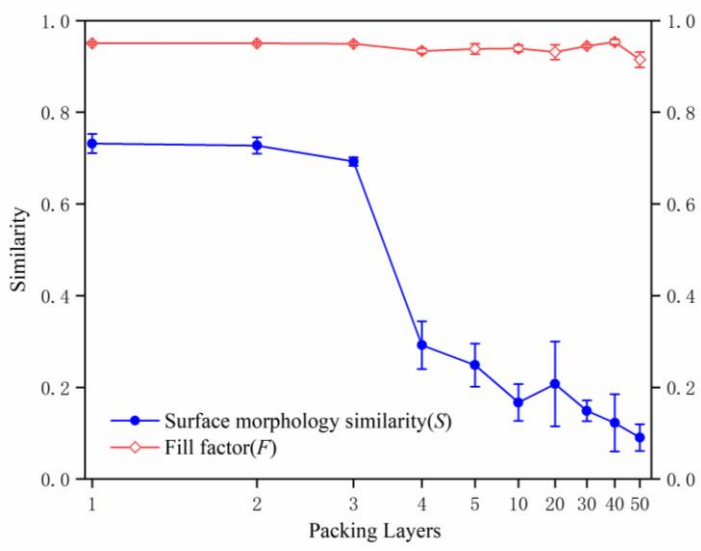

Figure 2. Dependence of surface morphology similarity and fill factor similarity on the number of packing layers.

Figure 2 indicates that increasing the number of packing layers leads to a notable rise in the dispersion of surface morphology, while exerting a minimal influence on the filling factor. For samples with three or fewer layers,S remains high (0.7–0.74) with small error bars, suggesting low dispersion. Beyond three layers, Sdecreases markedly (0.1–0.3), accompanied by a rapid increase in error bars, indicating great variability in surface morphology. In contrast, F remains stable at approximately 0.95, with narrow error bars indicating low dispersion and minimal dependence of the overall packing density on the number of layers. The stability of the packing density presents a counter-intuitive finding that challenges classical theory. This phenomenon can be explained by gravitational settling: a mechanism that consistently drives the fill factor toward its theoretical maximum, resulting in dense packing regardless of layer number.

3. Sample Preparation

This study introduces an innovative constrained droplet method for sample preparation, which enables the fabrication of multi-layer packing samples consistent with computational models by precisely controlling both particle size and arrangement, as illustrated in Figure 3. The preparation begins with multi-stage sieving using molecular sieves to obtain particles with a narrow, well-defined size distribution of 10 μm, corresponding to the computational setup. The total number of particles is then determined using the equal-circle packing in a circle (ECPC) theory [21]. Subsequently, a particle/alcohol solution at a specific concentration is prepared and subjected to 30-minute ultrasonication in a 120W water bath to ensure homogeneous mixing. A defined volume of the homogeneous suspension is deposited into the inner cavity of a zirconia substrate using a micropipette. A highly ordered monolayer forms via the facilitated self-assembly of aluminum particles under the combined effects of surface tension and gravity. Samples with packing layers of 1, 2, 3, 4, 5, 10, 20, 30, 40, and 50 were fabricated with five replicates each to align with the simulation parameters. Laser ignition experiments were then conducted on all samples under consistent conditions.

 doi:10.20944/preprints202605.0605.v1

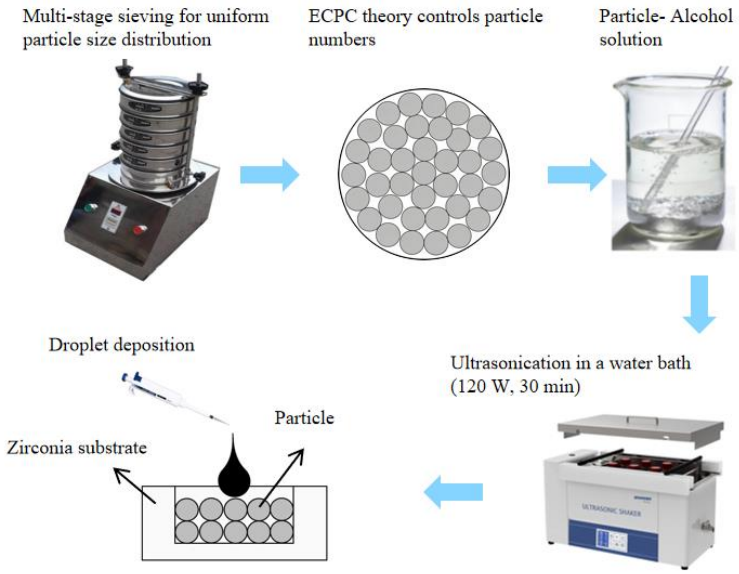

Figure 3. Constrained droplet sample preparation process.

To ensure consistency between the packing arrangement of experimental samples and computational models, careful control of particle shape and size is essential. Aluminum particles were selected as the fuel material in this study due to their well-established use in combustion and energetic materials research. The spherical aluminum powder, supplied by Henan Yuanyang Powder Technology Co., Ltd., exhibited a high degree of sphericity, as confirmed by scanning electron microscopy (SEM) images (Figure 4 (a)), thereby satisfying the morphological requirements. However, laser particle size analysis (Figure 5) revealed a broad size distribution ranging from 3 to 30 μm, with an average diameter of 10 μm. Such a wide size distribution not only leads to deviations in the packing structure compared to the computational models but also introduces significant variability in combustion behavior, adversely affecting the reproducibility of experimental results. According to the classical combustion law proposed by Glassman [22], which relates combustion time (t) to particle diameter (D_P) as $t \propto D_P^2$, the observed size variation can result in up to approximately 900% difference in combustion time, underscoring the critical need for strict particle size control. A multi-stage molecular sieving process with graded apertures was applied to the raw aluminum powder to eliminate coarse and fine outliers, resulting in a monodisperse ensemble. Post-sieving characterization confirmed the effectiveness of this treatment: SEM images (Figure 4 (b)) showed improved size uniformity, and laser particle size analysis (Figure 5) indicated a sharp, unimodal distribution within the 7–13 μm range, determined to be optimal through systematic experimentation.

Particles with sizes within the range where the probability distribution decays to $1/e$ of its maximum value are considered to have high statistical occurrence probability. Analysis of Figure 5 reveals that the combustion time of the raw particles deviated from that of the average-sized particle by a wide margin of -60% to 156%. Post-sieving, the deviation was confined to -24% to 21%, which corresponds to the minimum combustion error (approximately 21%) observed in subsequent experiments. The minimal impact of combustion duration deviation on the overall experimental inconsistency indicates that refining the particle size distribution is highly effective in suppressing combustion variability.

 doi:10.20944/preprints202605.0605.v1

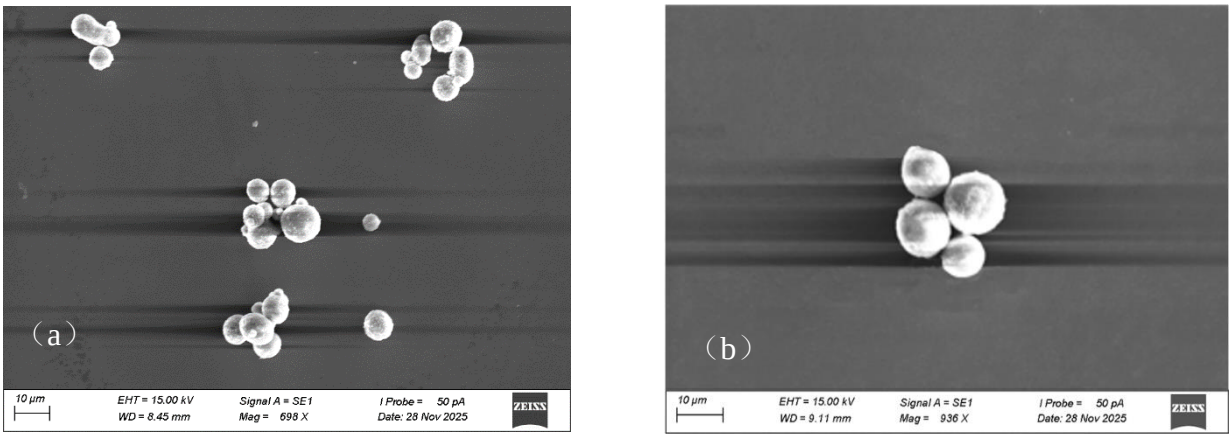

Figure 4. SEM images of aluminum particles :(a)before sieving; (b)after sieving.

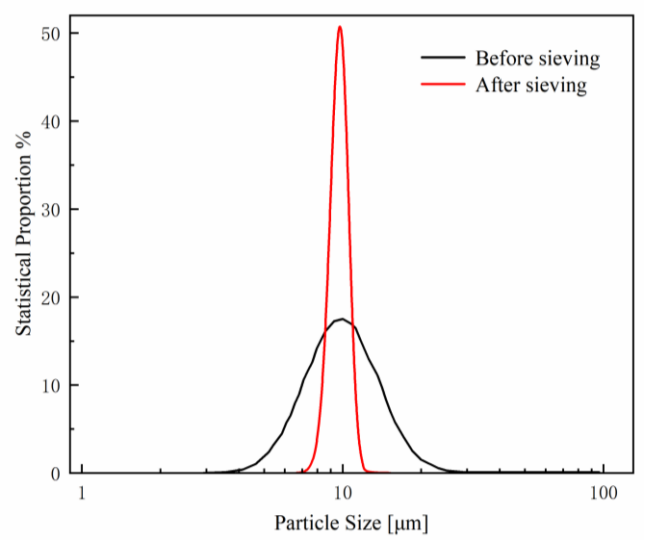

Figure 5. Particle size distribution curve before and after sieving.

Precise control over the number of layers in a packed sample requires careful design of the total number of particles, the core of which lies in determining the theoretical number of particles contained in a single layer. The ECPC theory provides an optimal solution to this problem. As a classical mathematical approach to two-dimensional dense packing, this theory yields the densest possible arrangement of identical particles within a larger circle without overlap. For a circle with an diameter of 2.5 mm and aluminum particles with an average diameter of 10 µm, the maximum number of particles accommodable in a single layer, 56600, can be derived from this packing theory. The total number of particles required is then calculated as 56600 multiplied by the number of packing layers. Based on this total, an aluminum/alcohol suspension with an appropriate concentration is prepared to supply the raw material for the constrained droplet sample preparation method.

Sintered dense zirconia was selected as the substrate due to its low thermal conductivity and high density, which collectively provide a consistent thermal environment for combustion experiments. Through hot-press sintering, zirconia achieves high densification (exceeding 95% of theoretical density), minimizing pores and defects to ensure uniform heat transfer. The effectiveness of this material for studying aluminum particle combustion interactions is well-established [23].

4. Laser Ignition Experiments

 doi:10.20944/preprints202605.0605.v1

In-situ flame radiation spectra were diagnosed using a laser ignition platform to reveal the determinants of experimental consistency, with the system diagram shown in Figure 6. The system comprises three main modules: a laser ignition unit, a spectral diagnosis unit, and a central signal generator for synchronization. A 980 nm semiconductor laser, coupled with a beam expander, constitutes the ignition source, producing a 3 mm diameter spot to ensure full coverage of the 2.5 mm diameter sample. For diagnostics, an optical fiber collects flame emission spectra and transmits them to a spectrometer. The relative positions of the sample and optical fiber were maintained constant across all experiments to enable quantitative spectral comparison. Synchronization of the laser and spectrometer is achieved by the signal generator, ensuring precise timing control. All experiments were conducted at room temperature and atmospheric pressure, with the laser operating at 200 W for 1.5 s. The spectrometer was configured with a 3 ms sampling interval and a 100 μs exposure time.

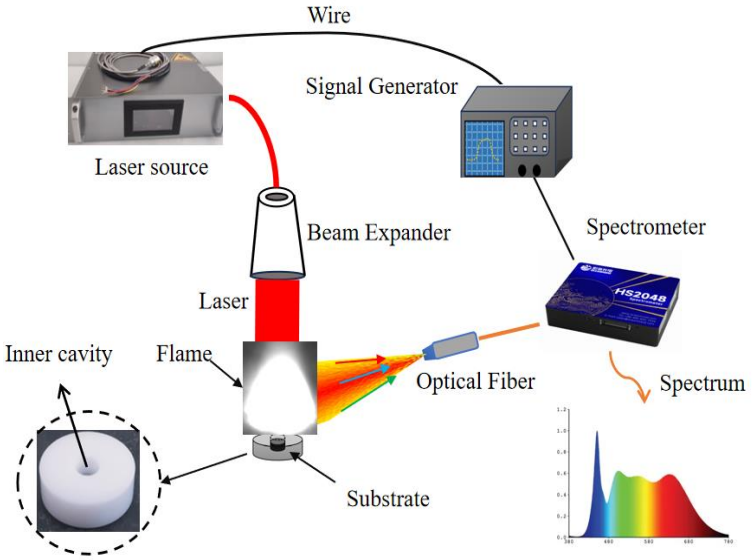

Figure 6. The schematic diagram of laser ignition system.

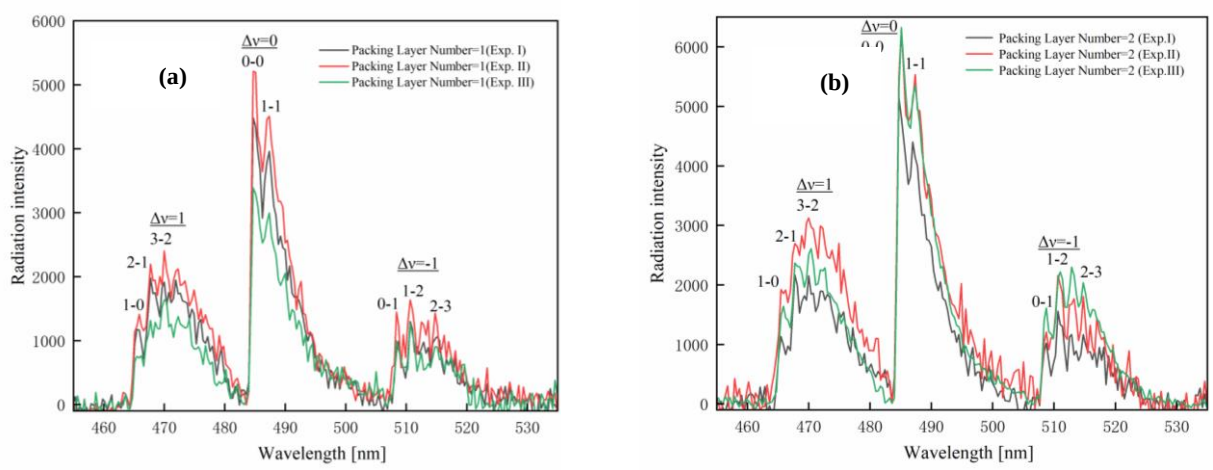

 doi:10.20944/preprints202605.0605.v1

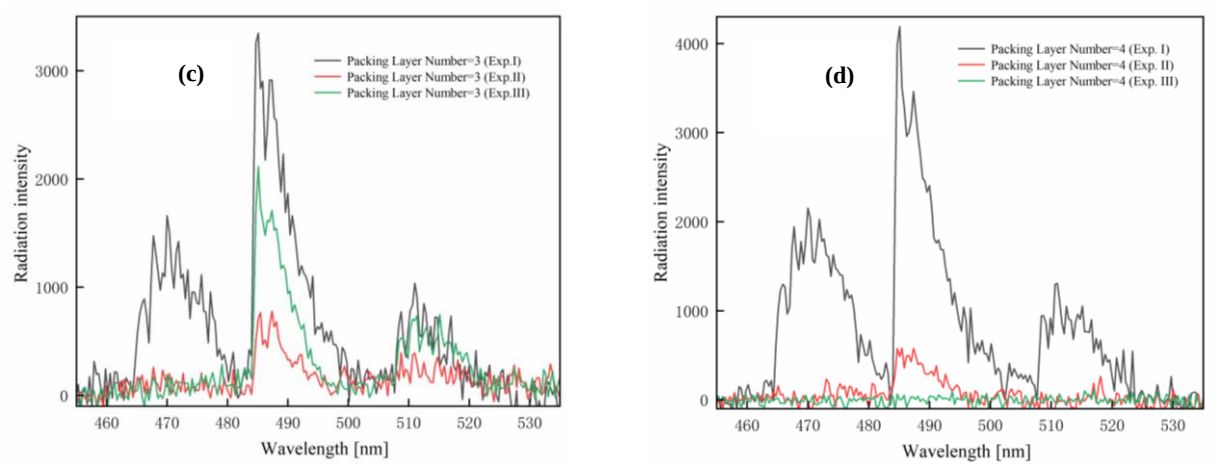

Figure 7. Spectral profiles of the AlO radical emission band (464.4–513.3 nm) recorded at 100ms without intensity correction, where Δv denotes the net change in the vibrational quantum number, while the v'-v" notation indicates a specific vibronic transition between defined vibrational energy levels. Results from three independent experimental trials for samples with (a) 1, (b) 2, (c) 3, and (d) 4 packing layers.

Laser ignition tests were conducted on samples with packing layers ranging from 1 to 50, with each configuration replicated five times. The combustion process was monitored by tracking the AlO radical's radiation band within the 464.4~513.3 nm wavelength range, a well-established diagnostic signature for aluminum combustion, Zhi ming P et al [24]. For direct comparison with the computational results, which were simulated for 1 to 4 layers, the spectral data presented in Figure 7 are limited to this corresponding range.

Figure 7 shows the characteristic spectrum of the AlO radical, where the main transition bands match previously reported results [citation:X], thereby validating the experimental approach. Analysis of the temporal spectral data further indicates that the consistency of the AlO spectrum at a given time decreases significantly with increasing packing layers. Importantly, this observed decline in spectral reproducibility correlates strongly with the corresponding decrease in surface morphology consistency. The spectral consistency of AlO significantly improves as the packing layers increase from 1 to 2. However, a rapid decline in consistency is observed when the layer count further increases to 3 and above. Due to the semi-quantitative nature of radiation intensity, which lacks directly comparable absolute values, the full width at half maximum (FWHM) of specific emission peaks is commonly employed as a metric for evaluating spectral consistency, Qing guo Z et al [25]. Among these, the $\Delta v = 0$ band—particularly the 0–0 band transition—is selected as the AlO characteristic peak owing to its highest radiation intensity. The temporal evolution of the FWHM of this AlO characteristic peak is tracked throughout the combustion process, forming what is termed the 'AlO characteristic FWHM curve'. To quantitatively assess the reproducibility of spectra across multiple experiments, the curve similarity function S is applied again to evaluate the consistency of AlO characteristic FWHM curve during combustion, and the results are shown in Figure 8.

 doi:10.20944/preprints202605.0605.v1

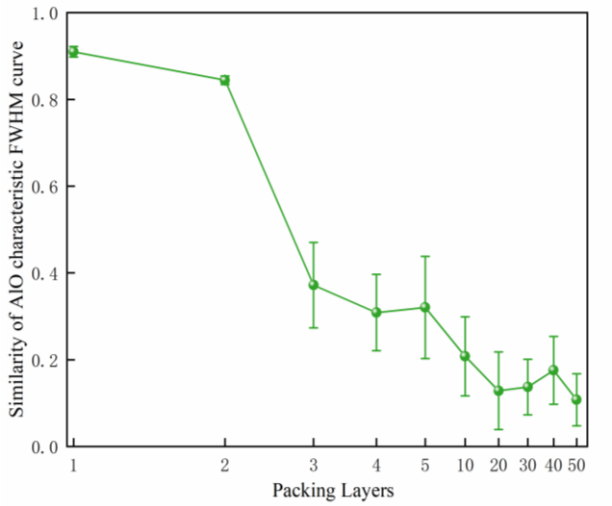

Figure 8. Dependence of AlO characteristic FWHM curve similarity on the number of packing layers.

Figure 8 illustrates a rapid decline in the consistency of the AlO characteristic spectral FWHM curve as the number of packing layers increases—a trend that closely mirrors the variation in surface morphology consistency. This correlation suggests that the uniformity of the surface layer predominantly governs the spectral consistency of AlO emission. When the stacking layer number is 1 or 2, the similarity function of the AlO spectrum remains above 0.85, accompanied by minimal error bars. In contrast, as the layer count exceeds 3, the similarity drops sharply to 0.1- 0.4, while the error bars expand significantly, often exceeding 50% of the mean value. Notably, the AlO spectral consistency shows a distinct degradation threshold at 3 layers—one layer fewer than the corresponding threshold for surface morphology consistency (4 layers). This discrepancy may be attributed to the fact that the two-dimensional computational model underestimates the actual three-dimensional packing consistency, particularly in capturing the increased morphological complexity and fluctuation introduced by additional dimension.

In combustion diagnostics using emission spectroscopy, the AlO characteristic peak intensity serves as a key factor for determining the ignition delay and combustion duration of samples. It has been widely observed that the AlO characteristic peak exhibits two distinct high-intensity regions: the first region appears within a narrow timeframe, while the second persists for a significantly longer duration [26]. The ignition delay is defined as the interval from the laser ignition point to the peak intensity of the first high-intensity region. The combustion duration is measured as the time interval between the 50% rise point and the 50% fall point of the second high-intensity region. The consistency of the experimentally determined ignition delay and combustion duration, as functions of packing layers, is presented in Figure 9 and Figure 10, respectively.

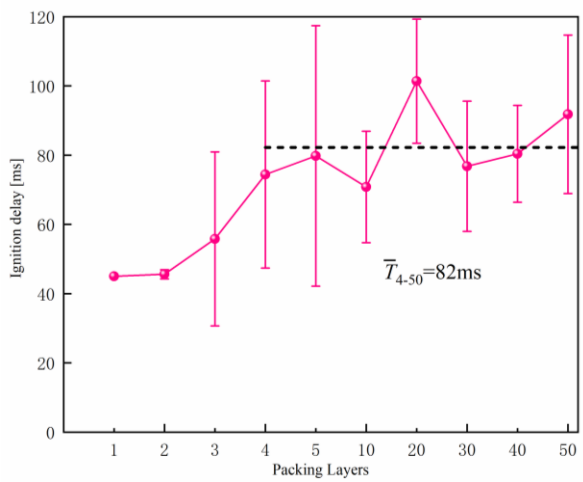

 doi:10.20944/preprints202605.0605.v1

Figure 9. Dependence of ignition delay similarity on the number of packing layers.

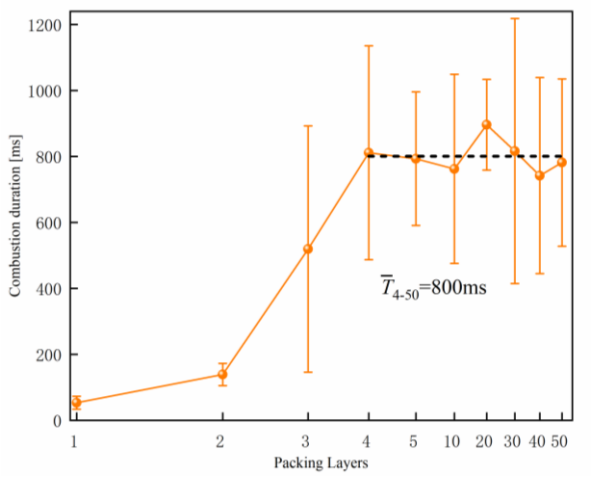

Figure 10. Dependence of combustion duration similarity on the number of packing layers.

As shown in Figure9 and Figure 10, the consistency of both ignition delay and combustion duration decreases rapidly with an increasing number of packing layers—a trend that closely mirrors the decline in surface morphology conformity. This strong correlation supports the conclusion that the reproducibility of combustion processes is predominantly governed by the consistency of surface morphology rather than variations in bulk packing density. Quantitatively, samples with 1 and 2 packing layers exhibit excellent experimental reproducibility, as reflected by small error bars in ignition delay (less than 4%) and combustion duration (less than 21%). However, a marked deterioration in consistency occurs when the number of layers exceeds 3. For packs ranging from 3 to 50 layers, the maximum scatter in ignition delay stabilizes in the range of 25%–50%, while that for combustion duration remains between 40% and 70%. Such significant data dispersion substantially undermines the reliability and analytical utility of the measured parameters, a phenomenon commonly encountered in randomly packed samples. It should be emphasized that these findings are established within the specific context of laser ignition. Whether surface morphology consistency remains the dominant factor under other heating regimes warrants further investigation.

The study further demonstrated that the constrained droplet method enables the measurement of key combustion parameters—such as the upper limits of average ignition delay and combustion duration, as well as the maximum penetration distance of heat flux—which are difficult to obtain using conventional random packing techniques. The observed trend—where the average ignition delay and average combustion duration increase initially and then plateau with additional packing layers under stable heating—is attributed to the heat transfer dynamics within the pack. For non-self-sustaining combustion (like aluminum particles), these processes rely on heat flux propagation, which is limited by factors like phase changes, reaction energetics, and product diffusion, and heat transfer during the laser duration. This limitation establishes a maximum penetration distance for effective heating, thereby capping the ignition delay and combustion duration.

Figure 10 indicates that the average combustion duration stabilizes at approximately 800 ms for packs exceeding 4 layers, with a maximum variation of about 10% across different layer counts. This trend suggests that under continuous 200 W laser irradiation lasting 1.5 s, the maximum penetration distance of heat flux during the combustion stage is approximately 40 μm. Given that the heat flux during the ignition stage is lower than during combustion—due to the absence of reaction exothermicity—the corresponding heat penetration distance during ignition is expected to be less than 40 μm. This further implies that the average ignition delay should also approach a maximum once the number of layers exceeds 4, a conclusion supported by the experimental observation. A comparison reveals that while the dispersion in average ignition delay decreases beyond 4 layers (with an upper limit of 82 ms), its maximum deviation across different layer counts exceeds 30%,

 doi:10.20944/preprints202605.0605.v1

which is significantly greater than that for combustion duration. The primary reason for this increased uncertainty is the relatively large particle size used in the ignition delay measurements. Since the average ignition delay recorded is about one-eighth of the average combustion duration, the particle size for the delay tests should theoretically be one-eighth of that for the combustion time tests to attain commensurate precision. Hence, applying the same particle size for both measurements, as in this study, results in poorer convergence for the ignition delay data due to this fundamental scaling rationale.

5. Conclusion

The major challenge in laser-ignited packing combustion research is the poor reproducibility of experimental results obtained from classical random packing sample preparation methods. To address this issue, the present study employed an integrated methodology of computational prediction, precision sample preparation, and experimental verification, leading to the groundbreaking conclusion that surface morphology, rather than overall packing density, is the decisive factor governing laser-ignition experimental reproducibility.

A two-dimensional DEM for multi-particle random packing was developed to simulate the semi-regular packing process. The simulation results revealed that increasing the number of packing layers leads to a significant decrease in the conformity of surface topography beyond 4 layers, whereas the overall packing density remains virtually constant. This apparent insensitivity of packing density to the number of layers contrasts with classical theory and is attributed to gravitational settling, which compacted the particle bed, causing the packing fraction to consistently approach the theoretical maximum.

An innovative constrained droplet method was proposed for fabricating semi-regular packing samples that closely mirror the computational models. This technique integrates multi-stage molecular sieving to narrow the size distribution of spherical aluminum particles, applies the ECPC theory to control the total number of particles precisely, and utilizes droplet deposition to build up the desired number of packing layers accurately.

A dedicated laser ignition platform was established to perform in situ diagnostics of the flame emission spectra from the packed aluminum samples. The influence of the number of packing layers on the consistency of four key combustion metrics—the AlO spectral profile and its characteristic FWHM curve, ignition delay, and combustion duration—was systematically investigated. The experimental results demonstrated that the consistency of all these parameters declines markedly when the number of layers exceeds 3. This trend closely mirrors the computational prediction of decreasing surface morphology conformity with increasing layers, robustly supporting the hypothesis that surface morphology consistency dictates experimental reproducibility under laser irradiation.

Furthermore, the constrained droplet method enabled the precise quantification of key combustion thresholds, including the average ignition delay, average combustion duration, and heat flux penetration distance. Notably, characterizing ignition-related thresholds required the use of smaller particle sizes than those employed for combustion-related parameters. These measurements—particularly challenging to obtain via conventional approaches—provide valuable input for precision numerical simulations.

In summary, this work challenges the conventional wisdom that packing density governs experimental reproducibility, and redefines surface morphology uniformity as the dominant controlling mechanism in laser-ignited combustion of random particle packings. These findings provide a foundational insight for advancing precision sample preparation methodologies, enabling the accurate determination of key combustion parameters previously obscured by conventional techniques, and ultimately clarifying the underlying physicochemical mechanisms governing particle ignition and combustion.

 doi:10.20944/preprints202605.0605.v1

Funding: The work was supported by the National Key Laboratory of Shock Wave and Detonation Physics (Grant No. 2024CXPTGFJJ06408), National Natural Science Foundation of China (Grant No. 11902276); National Key Laboratory of Computational Physics (Grant No. JK2025-04); Fundamental Research Funds for the Central Universities (Grant No.2682025ZTPY002).

Data Availability Statement: The original contributions presented in this study are included in the article. Further inquiries can be directed to the corresponding author.

Acknowledgments: The authors are grateful for the language polishing supported by Artificial Intelligence YuanBao.

Conflicts of Interest: The authors declare that they have no known competing financial interests or personal relationships that could have appeared to influence the work reported in this paper.

References

1. Y. Bai, H. Chen, X. Wu, W. Yang, F. Zhu, K. Chu, Y. Ba, Euler-Lagrange simulation of massive aluminum particles and agglomerates combustion in a realistic solid rocket motor environment, Powder Technology, 468 (2026).
2. F. Peng, H. Liu, W. Cai, Combustion diagnostics of metal particles: a review, Measurement Science and Technology, 34 (2023).
3. Z. Hu, Y. Feng, W. Dong, Y. Tang, J. Li, L. Liao, M. Zhao, B. Shi, Comprehensive modeling of ignition and combustion of multiscale aluminum particles under various pressure conditions, Chinese Journal of Aeronautics, 37 (2024) 188-202.
4. M. Beckstead, B. Newbold, A Summary of Aluminum Combustion, RTO/VKI Special Course on "Internal Aerodynamics in Solid Rocket Propulsion, (2004).
5. F.C. De Lucia, S.W. Dean, J.L. Gottfried, Commercial aluminum powders, part II: Energy release rates induced by rapid heating via pulsed laser excitation, Powder Technology, 399 (2022).
6. C. Felber, M. Köberl, E.A. Jägle, Powder bed fusion – Laser beam in reactive atmospheres – Ignition limits for Fe and Ti-6Al-4V powder blends in CO2 and N2, Powder Technology, 456 (2025).
7. S. Zhu, Y. Huang, L. Li, X. Wei, B. Liu, Research on laser induced plasma ignition of gas oxygen/methane, Acta Astronautica, 217 (2024) 208-220.
8. A. Zhakeyev, P. Wang, L. Zhang, W. Shu, H. Wang, J. Xuan, Additive Manufacturing: Unlocking the Evolution of Energy Materials, Advanced Science, 4 (2017) 1700187.
9. S.M.J. Endraß, T.M. Klapötke, J.T. Lechner, J. Stierstorfer, Application of 1- and 2-propargyl-tetrazole in laser-ignitable energetic coordination compounds, FirePhysChem, 3 (2023) 330-338.
10. M.W. Beckstead, Correlating aluminum burning times, Combustion, Explosion and Shock Waves, 41 (2005) 533-546.
11. A. Averardi, C. Cola, S.E. Zeltmann, N. Gupta, Effect of particle size distribution on the packing of powder beds: A critical discussion relevant to additive manufacturing, Materials Today Communications, 24 (2020).
12. N. Y, Y.q. Q, H. B, Relationship between laser ignition delay time and charge density of of Zr/$KClO_4$, Chinese Journal of Energetic Materials, (2008) 487-489.
13. B. Bockmon, M. Pantoya, S. Son, B. Asay, J. Mang, Combustion velocities and propagation mechanisms of metastable interstitial composites, Journal of Applied Physics, 98 (2005).
14. M.L. Pantoya, V.I. Levitas, J.J. Granier, J.B. Henderson, Effect of Bulk Density on Reaction Propagation in Nanothermites and Micron Thermites, Journal of Propulsion and Power, 25 (2009) 465-470.
15. N.T. Bharat, D.P. Mishra, The effect of disorderness in 2D adiabatic heterogeneous solid combustion under unstable and quenching regimes, Combustion Theory and Modelling, 29 (2025) 541-568.
16. V.A. Babuk, V.P. Belov, V. Khodosov, G.G.e. Shelukhin, Study of the structure of agglomerates with combustion of aluminized mixed condensed systems, Combustion, Explosion and Shock Waves, 24 (1988) 552-557.
17. O.B. Nazarenko, A.I. Sechin, A.A. Sechin, Y.A. Amelkovich, Flame propagation behavior of aluminum nanopowder in bulk layer, Journal of Loss Prevention in the Process Industries, 69 (2021).

 doi:10.20944/preprints202605.0605.v1

18. N. Kamaraj, C. Ghoroi, D.S. Sundaram, Influence of Particle Size and Packing Density on Combustion of Compacted Nickel-Aluminum Powder Mixtures, Combustion Science and Technology, 197 (2024) 6552-6579.
19. H. Kruggel-Emden, M. Sturm, S. Wirtz, V. Scherer, Selection of an appropriate time integration scheme for the discrete element method (DEM), Computers & Chemical Engineering, 32 (2008) 2263-2279.
20. A. Efrat, Q. Fan, S. Venkatasubramanian, Curve matching, time warping, and light fields: New algorithms for computing similarity between curves, Journal of mathematical imaging and vision, 27 (2007) 203-216.
21. K. He, H. Ye, Z. Wang, J. Liu, An efficient quasi-physical quasi-human algorithm for packing equal circles in a circular container, Computers & Operations Research, 92 (2018) 26-36.
22. I. Glassman, R.A. Yetter, N.G. Glumac, Combustion, Academic press2014.
23. C. Luo, Z. Yi, Q. Liu, F. Liu, W. Guo, H. Pei, X. Li, Investigating the Interaction Mechanisms of Aluminum Particles in Laser-Induced Ignition Experiments, Propellants, Explosives, Pyrotechnics, 50 (2025) e12030.
24. Z.m. P, Q.s. Y, C. L, N.y. Z, Z.l. J, Study on the radiation spectra of AlO radical B2Σ+-X2Σ+ and C2Πr-X2Σ+bands on the shock tube wall, spectroscopy and spectral analysis, 30 (2010) 865-868.
25. Q.g. Z, H.j. Y, J. H, The physical mechanism of spectral line broadening and its full width at half maximum, Journal of Henan University of Science and Technology (Natural Science Edition), (2008) 84-87+112.
26. C. Badiola, R.J. Gill, E.L. Dreizin, Combustion characteristics of micron-sized aluminum particles in oxygenated environments, Combustion and Flame, 158 (2011) 2064-2070.